

RNA Structure and Folding

Samuela Pasquali

Summer 2001

RNA is a biopolymer belonging to the class of nucleic acids. It is synthesized by the RNA polymerase as it travels along the DNA and copies its sequence. There are different kinds of RNAs performing different biological functions. mRNA carries the sequence information for protein synthesis to the ribosomes. Its primary sequence has a function while the secondary structure is much less important. tRNA brings the different aminoacids to the ribosome through the codon-anticodon mechanism. It is a short chain with a clover-leaf secondary structure which is by now well determined. rRNA is the ribosomal RNA that performs many catalytic tasks of the ribosome together with ribosomal proteins. In general a catalytic RNA is called a RNA-enzyme or a *ribozyme*. What enables rRNA to perform catalytic activities is the peculiarity of the tridimensional structure that it can assume. In this sense rRNA is similar to proteins that have to find the correct fold in order to be biologically active. With their ability to both store genetic information and participate in chemical reactions in the cell as enzymes, RNA molecules are believed to have played a central role in the origin of life and its early evolution, with DNA and proteins appearing only later. The aim of this presentation is to point out those features peculiar of RNA molecules that are believed to be related to their ability to fold, and to present the current knowledge on the folding mechanism. It is organized as a broad discussion focused on highlighting the general concepts more than the particular details of single RNA molecules, which can easily be found in the literature.

The first part of this work deals with the RNA structure and its organization at different levels of interaction, and with the folding process. Sections 1, 2, 3, 4 deal with RNA backbone, nucleotide pairing, secondary and tertiary structural motifs respec-

tively. Section 5 describes the folding process from the energetical and dynamical point of view. Section 6 focuses on the role played by metal ions and water in stabilizing the tridimensional structure.

The second part, Section 7, is a presentation of various models introduced to predict RNA secondary structure. Here also the goal is to understand the basic concepts involved in each scheme and their differences, more than the technical details needed to implement each one of them on a computer.

Section 8 presents the work by Carlos Bustamante and coworkers on the stretching experiments on long molecules. Their experimental approach, recently applied also to RNA molecules, can give useful insights on the specific transformations that are involved in the folding of a single molecule. To better explain the potential of the technique, this section includes a brief discussion of the previous studies on DNA and Titin molecule.

1 Backbone Structure

RNA chain has a sugar-phosphate-sugar-phosphate backbone with the bases Adenine A, Uracile U, Cytosine C, and Guanosine G as side chains, where U is the pyrimidine that plays the same role as Timine T does in DNA. RNA molecules are typically made up of 10 to 1000 bases, they are therefore much shorter in length than typical DNAs. There are both double stranded RNA molecules and single stranded RNA molecules, the latter being particularly interesting due to their ability to fold to a well specified 3D structure.

RNA is formed by β -D-ribosyl nucleotides. β indicates that the c5' and the base are on the same side with respect to the ribose ring. The ribose sugars are about in a c3'-endo conformation, i.e. c3' is out of the plane of the sugar ring, and it is on the same side as the c5' and the base. In general both c3' and c2' will not be on the plane and their displacement off the plane is about 0.5 Å or less.

Chemically RNA differs from DNA only in the absence of a methyl group at position 5 of Uracil and in the presence of an OH instead of H at 2' of the ribose sugar. One consequence of the presence of the OH group is that RNA is more susceptible of hydrolysis and is less flexible than DNA. This steric constraint doesn't allow RNA to

form B helices, but allows only A-form conformations [Figure 1]. RNA in helical form is not affected by changes in the environment and adopts the A helical form under nearly all conditions [1].

An A-form helix is a right handed helix that can occur with any sequence. It is thick and compressed along the helix axis. The numerical values characteristic of an A-form helix are given below [2, 3]; the number in parenthesis refer to the B-form helix

Rise per base pair	2.3 $\overset{\circ}{\text{Å}}$	(3.32)
Helix-packing diameter	25.5 $\overset{\circ}{\text{Å}}$	(23.7)
Base pair per turn of helix	~ 11	(~ 10)
Mean rotation per base pair	33.6 $^{\circ}$	(35.9)
Pitch per turn of helix	26.6 $\overset{\circ}{\text{Å}}$	(32.2)
Tilt	+19 $^{\circ}$	(-1.2)
Propeller twist	+18 $^{\circ}$	(+16)

Having given this numbers it is important to notice that helical parameters vary a lot, allowing for specific recognition and binding to proteins and drugs.

The two grooves in an A-form helix have almost the same width, but one is deep and one is shallow. One therefore talks of "shallow groove" and "deep groove" instead of major and minor groove like for DNA. The accessibility of the shallow groove allows functional groups, particularly the 2' OH group of the ribose, to participate to interactions. The importance of the shallow groove in mediating tertiary interactions may be a fundamental reason why RNA folds into complex tridimensional structures while DNA doesn't.

In RNA, stacking plays a particularly important role in stabilizing the helical structure (the other essential interaction being hydrogen bonding) and the 3D structure in general. The dominance of stacking in stabilizing RNA structure is demonstrated by tRNA in which only 41 out of 76 bases are involved in helical structure, but 72 bases are involved in stacking interactions [4]. In an A-form helix the way one base pair stacks to the next depends on the specific sequence, and the stacking energy is sensitive to local changes in relative orientation of neighboring base pairs. Stacking of bases occurs predominantly between consecutive residues within one strand, but also other phenomena like intercalation of one base into the helix can occur.

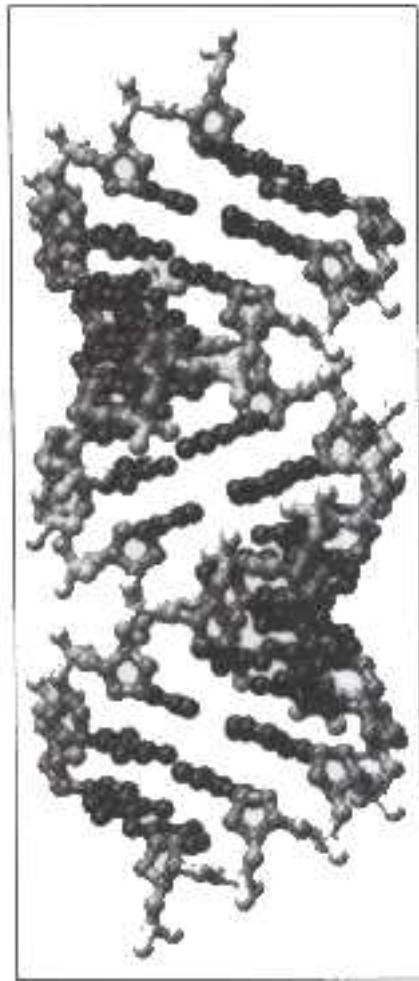


Figure 1: Representation of a A-form helix. The shallow groove can be seen in the upper left corner and lower right corner of the figure, while the deep groove can be seen in the two opposite corners.

The conformation of each nucleotide depends on the torsion angle for rotation around each backbone bond. Bond stretching and bond-angle bending also occur but they are less important (typically occur at much higher energies). There are 7 torsion angles per nucleotide (7 degrees of freedom) which allow a base to position itself in almost any orientation making it possible to form base pairing outside the helix and to form multi-base hydrogen bonding (base triplets or even quadruplets).

2 Nucleotide Pairing

Each base has three edges that can be used for pairing: the Watson-Crick edge, the Hoogsteen edge and the shallow groove edge [Figure 2].

W-C pairs are found in the helical part of the molecule, while Hoogsteen pairs are found in the formation of triple helices and in corners of tRNA structures. Shallow groove pairs are frequently observed in recognition elements in RNA-peptide/protein complexes [5]. Canonical W-C pairing rules predict hydrogen bonding between Adenin A and Uracil U, and between Guanin G and Cytosin C.

The usual definition of secondary structure includes also the G·U wobble pair. G·U pairs form two hydrogen bonds on the W-C edge of the bases, and are virtually as stable as A·U pairs. In the wobble G·U pairs the U points into the deep groove of RNA helix leaving a hollow surface in the shallow groove [Figure 3]. The cavity left free by U favorably stabilizes water molecules or other hydrophylic atoms [6]. By introducing a polar pocket, and thus a slight asymmetry in a regular helix, G·U pairs constitute points of deformability allowing the necessary conformational adaptation for promoting catalytic activity. The displacement of U provokes an asymmetry in the angles subtended at the glycosyl carbon c1'. This difference in angle is at the origin of the non-isostericity of G·U and U·G. Statistics on rRNAs indicate a preference for the stacked 5'-G·U-3' base pair over the opposite, at the end of helices. Thermodynamically also, helices ending with 5'-G·U-3' are more stable than helices ending with U·G. This can be explained observing that G·U and U·G have different stacking patterns [6]. Moreover G·U pairs are slightly less stable when they are in the middle of a W-C helix than when at an end. This is caused by the increase in the width (c1'-c1' distance) of a G·U pair with respect to a W-C pair and could account

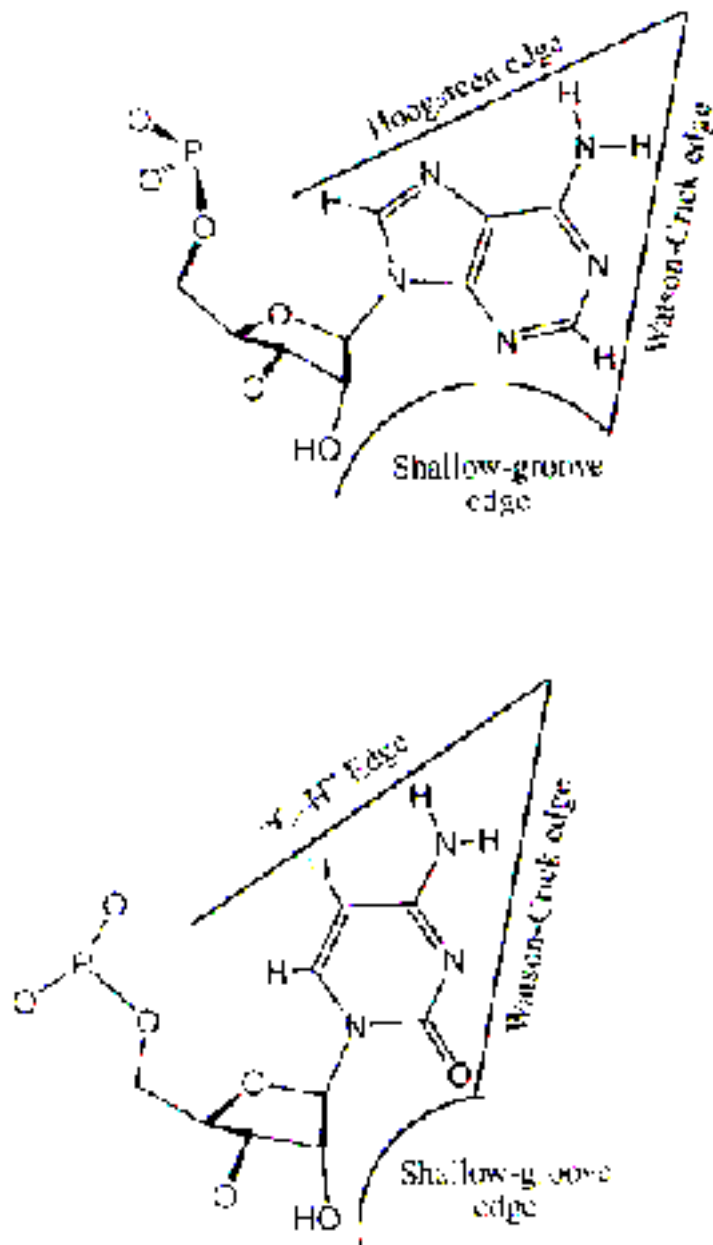


Figure 2: The three edges of purine A and pyrimidine C. The Hoogsteen edge in purine is replaced with the C-H edge in pyrimidine.

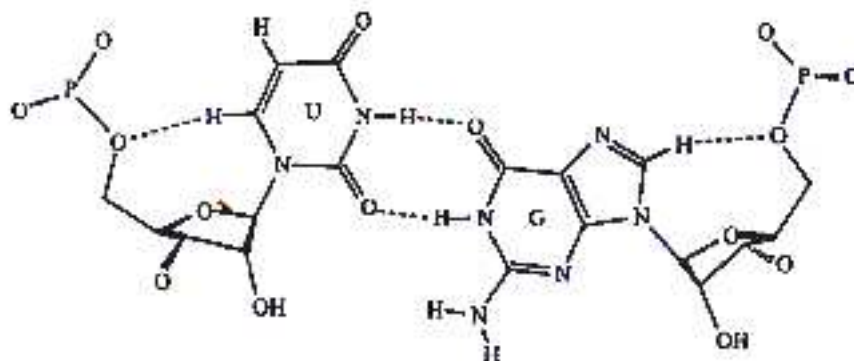


Figure 3: The wobble G·U pair. It involves the W-C edge of both bases, and as A·U it involves two hydrogen bonds.

for the fact that most G·U pairs are found at the end of helices. G·U pairs exchange most frequently with W-C pairs and with A·C pairs ($A^+ \cdot C$ pair is isosteric to G·U). Allowing the use of all three edges of the bases for hydrogen-bonding, brings to the formation of many different combinations of pairs. Moreover some pairs involve non-standard hydrogen-bonding rules, like bifurcation bonds, and participation of C-H bonds in some sort of hydrogen bonding, like C-H \cdots N. Some pairs are mediated by the insertion of one or more water molecules, like the water mediated G·A pairs where there is only one direct hydrogen bond, and G·A is sandwiched between two bifurcated bonds. Indeed non-canonical pairs that are connected by a single hydrogen bond require water molecules in order to obtain a stable base pairing scheme. Mismatched pairs participate in stacking interactions and provide recognition sites both by presenting functional groups at the base edges, and by distorting the regular helical backbone. Homopurine G·A mismatches are the most common non-canonical structural motifs in RNA molecules.

Unlike for DNA, in RNA molecules it is possible to have also the backbone interacting with the bases via hydrogen bonding, due to the shallowness of the minor groove that makes the backbone easily accessible. This involves the OH group at 2' of the ribose. Hydrogen bonds in the shallow groove all involve the 2' hydroxyl group. Adenosine is the base most frequently found to interact with the shallow groove edge of another base. In the cis W-C-shallow groove pair the N1 of A binds the OH group [5].

These are just a few examples of the diverse kinds of pairing that can occur in an RNA molecule; The reader is referred to [7] for an exhaustive description.

3 Secondary Structure

A base pair always has $j - i > 3$, i.e. there are at least 3 monomers between monomers i and j that are paired. This constraint comes from steric consideration on the RNA backbone that cannot make a U turn in less than three monomers.

Two base pairs (i, j) (h, k) , where $i < h$, are called:

nested if $i < h < k < j$

unrelated if $i < j < h < k$

linked if $i < h < j < k$

two linked base pairs form a "cross-link" or a pseudoknot.

RNA secondary structure is a set of base pairs in which no two base pairs are linked, that is, every base pair in a secondary structure is either nested or unrelated [8, 9]. This is equivalent to saying that the secondary structure can be represented by a planar graph in which no lines intersect [1, 10, 11] [Figure 4]. A more strict definition states that to the secondary structure belongs any nucleotide such that both itself and one at least of its immediate neighbors are involved in classical Watson-Crick base pairing with a stretch of nucleotides in anti-parallel orientation [1]. Not every set of pairs represents a valid secondary structure with chemical and stereochemical constraints eliminating most possibilities.

It is possible to classify basic secondary structures into: single stranded regions, hairpins, bulge loops, mismatches, internal loops, and junctions [10] [Figure 5].

Single stranded regions consist of unpaired nucleotides at the 5' or 3' end of the molecule, or between duplex regions of an RNA secondary structure. These regions are assumed to be roughly ordered by base stacking in a helical geometry.

Hairpins consist of a duplex bridged by a loop of unpaired nucleotides. Hairpin loops are known to bind to proteins, to form tertiary interactions, and serve as nucleation sites for RNA folding. The turn that originates the loop can be caused by a change in the phosphodiester torsion angle and can be stabilized by hydrogen bonds and stacking. The smallest loop is of 2-3 nucleotides, but loops containing 4 or 5 nucleotides

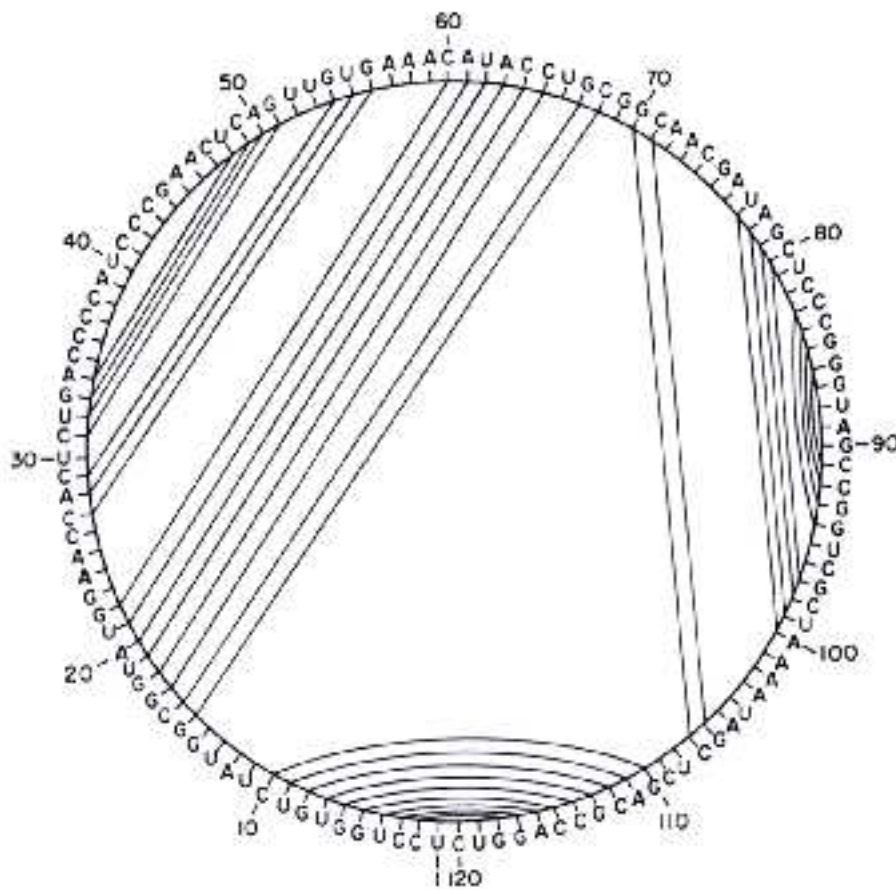


Figure 4: Representation of the secondary structure as a planar circular graph. All bases are indicated as a vertex on the external edge of the circle. Hydrogen bonds between nucleotides are indicated by chords connecting the two bases involved in the bond. Secondary structures are characterized by the fact that there are no two chords intersecting.

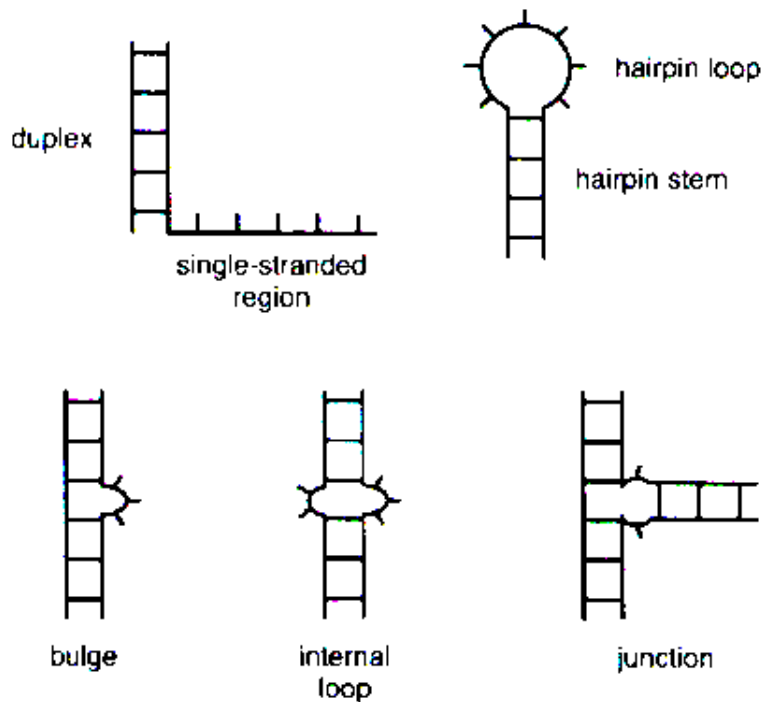


Figure 5: Secondary structure elements

are the most stable. For small loops the conformation of the sugar-phosphate backbone is very different from the A-form geometry. Some have a 2'-endo conformation, different from the 3'-endo conformation of the A-stem. Some of the loop backbone angles are different from the angles found in duplex regions. This differences with the A-form geometry seems to be a general feature of small hairpin loops. A-form geometry is instead preserved in portions of larger hairpin loops. The conformation of the nucleotides in small loops suggests that some of them are not very accessible for tertiary base pairing with other elements of the molecule, while nucleotides in loops that are in a normal A-form geometry are facilitated in pairing with other nucleotides external to the loop. In larger hairpins a considerable content of purines often allows extensive mismatch base interactions leaving only a few unpaired residues [12]. The stability of a hairpin loop changes with size and sequence. Out of all possible 4-base sequences for a tetraloop, only eight different 4-base-loop account for over 60 % of

the ribosomal tetraloops found [10].

Bulge loops consist of unpaired nucleotides on one strand of a double-stranded region while the other strand has continuous base pairing. The unpaired bases can intercalate into the helix or can be extra-helical. The equilibrium between a bulge nucleotide intercalating in or looping out the helix depends on temperature, identity of the bulge nucleotides and sequence of the base pairs surrounding the bulge. Bulges can affect the long-range structure of the molecule by creating bends in the double helix. Bends depend on the identity of the nucleotides and are also affected by the surrounding base pairs. One common assumption made when modeling RNA secondary structure [9, 13] is that it is independent of the surrounding conformations. In the case of bulges one needs to be particularly careful since bulge nucleotides affect the structure of the duplex surrounding them for several base pairs. Indeed the distortion introduced with the bulge it is not necessarily localized at the bulge site, but may extend into duplex regions near by.

Mismatches consist of two opposed nucleotides that cannot form a W-C base pair, they can engage in some other form of hydrogen bonding or they can form an open loop of two non-bonded nucleotides. The most characterized mismatch is the wobble G·U pair. A change in backbone conformation could be a recurring feature of mismatches, although these distortions seem to depend on the sequence surrounding the mismatch. When a mismatch occurs between bases inside a helix it doesn't seem to cause significant bends in the helix axis. Thermodynamically mismatches involving G are the most stable while the one involving C are the least stable.

Internal loops contain 3 or more nucleotides not capable of forming W-C base pairs and contain at least one unpaired nucleotide on each strand. The loops can close by forming non-canonical base pairing, or can remain open, allowing for easy engagement in tertiary interactions with other parts of the molecule. The accessibility of nucleotides in internal loops to tertiary pairing depends ultimately on the loop conformation. Extensive stacking of bases within open internal loops may facilitate tertiary pairing, whereas bases in a closed internal loop would be unavailable. Asymmetrical loops are thermodynamically less stable than symmetrical ones and their structure can be significantly different despite the insertion of just one additional nucleotide.

Junctions, or **multibranched loops**, contain 3 or more double-helical regions with

a variable number of unpaired nucleotides where the helical regions come together. The unpaired nucleotides in the junctions act as a hinge controlling how the helical regions stack on each other, thus determining the overall 3D conformation of the RNA molecule. It seems to be a general feature of junctions that different stems stack coaxially to form longer helical regions. Two known configurations for 4 stems junctions are the **X** and the **L**, typical of tRNA. It has been suggested that the helical regions separated by the fewest unpaired nucleotides will stack coaxially. In addition to stacking helical regions, junctions orient the different helical regions in space and appear to constitute catalytic sites. Coaxial stacking is often achieved through the binding of divalent metal ions near the site of the stack, and also the orientation of the helices with respect to one another is extremely sensitive to the concentration of divalent ions [4]. From the biological standpoint, junctions appear to constitute catalytic sites for RNA, where a particularly important role would be played by the unpaired nucleotides.

4 Tertiary Interactions

RNA molecules fold into compact structures stabilized by interactions not included in the secondary structure. Secondary and tertiary interactions are distinguished by chord crossing (refer to Figure 4). Tertiary interactions are considered separately from secondary interactions since their formation depends also on the rest of the secondary structure, and not only on the nucleotides strictly involved in the interaction. Most tertiary interactions involve non-canonical base pairing or backbone-backbone interaction. Some non-canonical motifs always found to be involved in tertiary interactions are: adenosine platforms, triples, tetraloops, helices packing, metal-core motifs, ribose zippers [4]. Adenosine platforms and triples involve non W-C pairing, tetraloops and helix docking involve non-canonical pairing as well as backbone-backbone or backbone-base interactions, ribose zippers involve backbone-backbone interactions.

Tertiary structures that involves W-C pairing are the pseudoknots and the kissing loops. Pseudoknots and loop-loop interactions tie together single stranded regions. Complementary loops can form **kissing complexes** in which all single stranded nu-

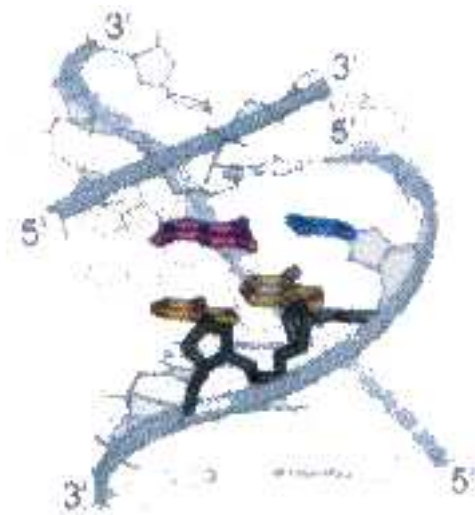


Figure 6: Adenosine platform. The interaction between consecutive coplanar bases within one strand gives rise to platforms that provide stacking surfaces for other bases. In this as well as in the following pictures the color coding is the following: orange for A, magenta for G, green for U, and blue for C.

cleotides are involved in base-pairing giving rise to a quasi-helical module. Triples can mediate helix-single stranded region interactions; tetraloops can bond with both single stranded or double stranded regions.

Adenosine platforms [Figure 6] consist of two sequential A groups arranged side-by-side to create a "pseudo base pair". An AA-platform motif, involves a cis Hoogsteen-shallow groove contact between subsequent bases. Each adenosine platform has a non W-C base pair immediately below it, either a G·U wobble pair or a Hoogsteen type A·U pair which creates a local distortion of the helix which enhances the stacking between the platform and the non-canonical pair. The other face of the platform remains free to participate in tertiary stacking interactions like in the tetraloop tetraloop-receptor interaction. Stabilization of adenosine platforms requires the presence of monovalent metal ions, preferably K^+ , which binds to a specific pocket immediately below the adenosine bases.

Triples [Figure 7]. Major groove triples involve a purine interacting with the Hoogsteen edge of a purine involved in a W-C pair. Minor groove triples involve an adeno-

sine, coplanar with a U·A reverse Hoogsteen base pair, forming a hydrogen bond with a 2'OH group. Both are stabilized by hydrogen bonding and stacking [10]. Extended single stranded regions appear to tie helical regions together through the formation of base-triple interactions. The formation of base-triples in junction regions where helices stack coaxially may be a recurring RNA structural element [10, 4]. Depending on the topological connection of the strand which provides the third base docking to the already existing pair, triples can lead to widened grooves within double stranded architectures, which facilitates the interactions with protein for example, or can mediate the tertiary interaction of an other strand [12]. A particular interaction mediated by the minor groove triples is the tetraloop-tetraloop receptor interaction.

Tetraloops [Figure 8] are among the most recurring motifs observed in natural RNAs. They are 4 nucleotides loop sequences, the majority of which fall in two sequence categories: UNCG and GNRA, N being any base, R being a purine A or G. GNRA is the most abundant tetraloop. A network of hydrogen-bonding and base-stacking interactions creates a stable structure. In all of these loops the G in position 1 and the A in position 4 form a shallow groove base pair in which the G-N3 hydrogen bonds with A-N6 and G-N2 hydrogen bonds with A-N7. In GAAA and GCAA the distance between G-N3 and A-N6 is too big for direct hydrogen bonding to occur and the interaction is likely to be water mediated. The two internal bases are stabilized by stacking interactions rather than hydrogen bonds. The fact that they are not conserved, like the second base in GNRA, indicates a role of the sugar backbone rather than of the base for the loop structure. Two particular tetraloop sequences, namely the already mentioned GAAA and UUCG, form an unusually stable hairpin. Interactions between loop bases and the sugar-phosphate backbone contribute to the unusual stability of these sequences. GNRA tetraloops form tertiary interactions in which the tetraloop receptor adopts a conformation consisting of two W-C G·C base pairs and reverse-Hoogsteen A·U base pair, an adenosine platform and a wobble G·U base pair [Figure 9]. Both the loop and its receptor can tolerate a high degree of variability without sacrificing binding affinity nor specificity.

Helices can pack both perpendicularly or parallel so that the backbone of one helix contacts the shallow groove of the other helix. Both arrangements are dominated by the 2' hydroxyl groups in mediating the interaction. For the perpendicular con-

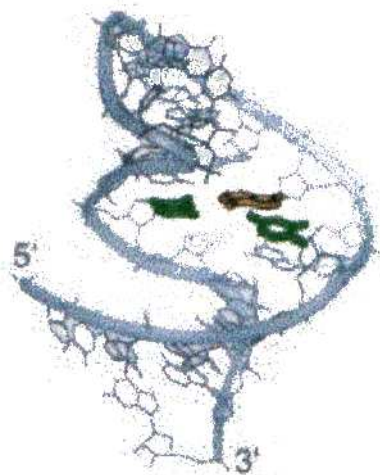


Figure 7: Base triple formed by two strands. The triple widens RNA grooves facilitating tertiary interactions as well as the interaction with proteins.

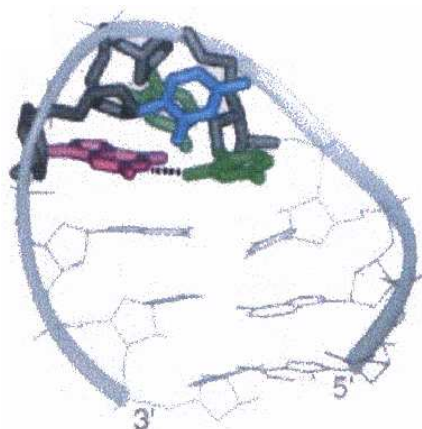


Figure 8: The UUCG tetraloop from the P1 hairpin of group I ribozymes. The hydrogen bond between the first and the last residue is visible. This interaction, together with extensive stacking is responsible for the high stability of the tetraloop of the UNCG family.

figuration at each site of contact extensive hydrogen bonding occurs between the 2' hydroxyl group, the 3' oxygen atom and the phosphate oxygen atom of the backbone of one helix and the pyrimidine O2 atom, the exocyclic amine of guanosine and the 2' hydroxyl group in the shallow groove of the second helix. When helices are parallel they make a limited number of interhelical contacts primarily through water-mediated backbone-backbone contacts and the 2' hydroxyl-phosphate contact. In general helix-helix interactions may include base-phosphate, base-sugar, sugar-sugar, and sugar-phosphate hydrogen bonding.

Metal-core motif [Figure 10]. Metal ions are integral parts of RNA architectures in which they occupy specific binding pockets. Metal cations are bounded either directly or by water mediated interactions. They can simultaneously interact with phosphate groups and bases tethering the backbone of single stranded regions with the groove of duplexes. Potentially unfavorable electrostatic interactions created by close packing of the phosphate backbone are relieved by bonding to a magnesium ion, like, for example, when the ribose-phosphate backbone of a bulge forms a corkscrew turn in which the phosphates are placed toward the interior and the nucleotides bases are flipped outward, in some group I introns. The nucleotide bases splayed out from the bulge are free to form tertiary contacts. The nucleotide sequence affects the ability of the backbone to specifically bind to metal ions. Examples of pyrimidine rich bulges bounded to Mg^{2+} are found in natural RNA [4].

Ribose zippers [Figure 11] occur when there is close contact between backbones. In the tertiary interactions mediated by the adenosine rich bulges and the GAAA tetraloop-tetraloop receptor, the two backbones come in close contact as two helices are docked against one another. At those sites the ribose sugars of antiparallel strands become interdigitated by the formation of bifurcated hydrogen bonds between the 2'-OH of a ribose from one helix and the 2'-OH and the N3 atom of a purine or the O2 atom of a pyrimidine in the opposite helix. This creates a zipper of ribose sugars in the shallow groove of the two helices that can potentially pack RNA strands and helices together with a few sequence-specific requirements. The local geometry of the hydrogen-bonding network is conserved among different RNAs, despite the dissimilarity of the conformations of RNA strands which are held together [12].

Pseudoknots [Figure 12] are defined as motifs in which nucleotides of a hairpin loop

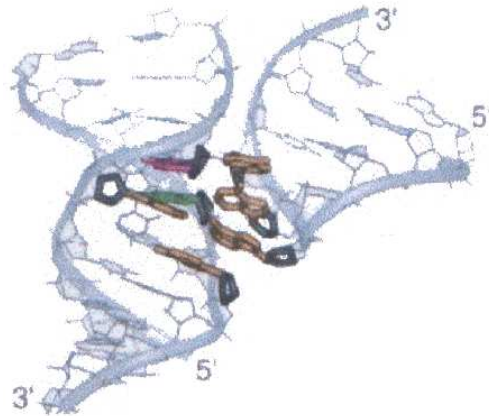


Figure 9: A GAAA tetraloop, from the P4-P6 domain of group I ribozymes, docks into a receptor module which provides stabilizing contacts by stacking, mismatch pairing and hydrogen bonding to the backbone.

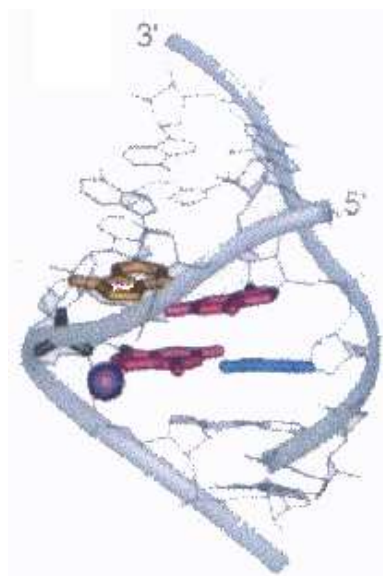


Figure 10: Divalent cation coordinated at the deep groove edge of a sheared G·A pair in an RNA duplex.

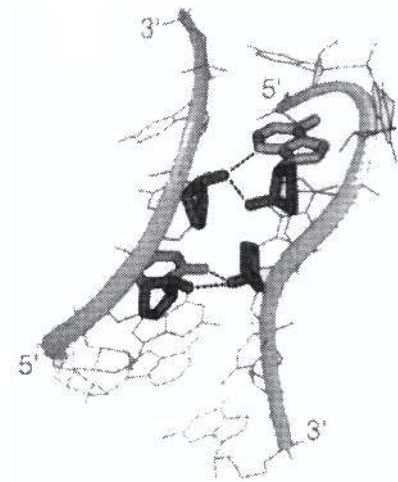


Figure 11: Ribose zipper. This particular arrangement is highly conserved despite the dissimilar overall structure of the two strands which are held together.

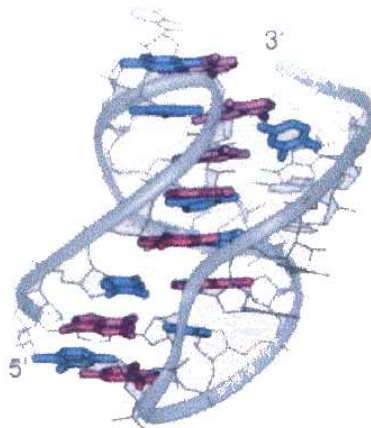


Figure 12: A simple pseudoknot configuration responsible for compact folding of RNA tertiary architectures.

base pair with a complementary single stranded sequence via W-C pairing. On one side it appears to be a normal duplex, while on the other side two loops bridge the duplex, one crossing the shallow groove, one crossing the deep groove. The classic pseudoknot consists of a hairpin loop pairing with a complementary sequence next to the hairpin stem to form a contiguous coaxially stacked helix. The pseudoknot is only marginally more stable than the competing hairpin structures that the same sequence could form [10]. The equilibrium between pseudoknots and hairpins depends on salt concentration, temperature and nucleotide sequence. To achieve complete stabilization pseudoknots usually require some binding to metal ions. They occur in either high Na^+ concentrations or Mg^{2+} solutions.

In addition to these motifs looping out of single residues is frequently found in hairpin loops and internal loops which are zippered up into compact structures by stacking and by the formation of mismatch pairs. Such "bulges in a loop" play a key structural role by introducing flexible hinges in the RNA backbone, providing recognition sites for proteins, and acting as "flaps" which close over a binding cavity. Intercalation of an unpaired nucleotide between base pairs is yet another way to introduce possible stabilization of tertiary architecture by stacking bases. In order to accommodate for intercalation the sugar-phosphate backbone can change conformation, for example to a 2'-endo [10].

5 Folding

A 3D architectural motif is a simple but recurrent association of a few secondary structure elements with specific geometrical and topological arrangement. A 3D motif occurs via interactions involving two helices, two unpaired regions or one unpaired region and a double-stranded helix. The motifs are the ones described in Section 4. There are three ways in which two paired segments can be related to each other: two consecutive hairpins, two helices separated by an internal loop or bulge, and pseudoknot [14]. W-C pairing between two unpaired regions normally leads to pseudoknots, while pairing of a single-stranded stretch, either in the deep or shallow groove of a double helix, yields a triple helix.

An RNA molecule can be thought of possessing a hierarchical structure in which

the primary sequence determines the secondary structure which in turn determines its tertiary folding, whose formation alters only minimally the secondary structure [15, 14]. 3D architecture results from the compaction of separate preexisting and stable elements, like the ones listed in Section 3, plus pseudoknots, that form autonomous entities. This reveals in the fact that RNA unfolds in a series of discrete steps corresponding to the breaking down of the folding process into localized regions of the structure.

Given a sequence, next-neighbor interactions lead first to regular structural elements of secondary structures and 3D motifs which subsequently merge into domains as structural units that fold separately. Pre-formed domains associate to form the compact tertiary structure without much reorganization (unlike what happens in protein folding).

The thermodynamics and the kinetics of folding are directly linked in RNA. Secondary structures are very stable with a $\Delta G = -1$ to -3 kcal/mol per base pair. Natural sequences melt at higher temperatures, and over narrower ranges, than random sequences, indicating that their 2D structures are more stable than if they were random, and their melting is a more cooperative process. A single base pair is never stable in aqueous solution since hydrogen bonding provides about 1 kcal/mol of stabilization which is not enough to counteract even the entropy of a loop composed of four nucleotides ($\Delta G(37^\circ) = +4.5$ kcal/mol). As a consequence consecutive base pairs must form in order to form a loop and this constitutes the first step in folding. Loops and bulges decrease the entropy of the single strand, so they form only if the free energy decrease of base pair formation exceeds the cost of loop closure. Larger hairpin loops can form if the loss in configurational entropy of closing the loop is compensated by increasing numbers of successive base pairs [15]. In the single strand RNAs the ends are far apart and the formation of the base pair among them would greatly decrease the entropy. Formation of base pairs between ends is thus kinetically and thermodynamically unfavored until most of the other parts have already formed. Eventually at low temperatures and/or high ionic strength the least stable structures involving tertiary interactions form.

The time it takes for a molecule to fold is dictated by the time it takes to rearrange the backbone. Indeed, stacking of isolated bases is diffusion controlled (time range

of 10 ns), while stacking of single stranded nucleotides is much slower because of the folding of the sugar-phosphate backbone (time range 1 μ s).

The partition into secondary and tertiary structure is challenged by studies of the unfolding pathway of a 113-nucleotide long pseudoknot [14, 16]. In this case melting of tertiary structure was not well separated from melting of secondary structure. Depending on molecule length, structural complexity, and the resulting relative stabilities of secondary and tertiary structures, it is legitimate to wonder whether secondary and tertiary base pairs (the way they are defined) always correspond to well spaced energy levels, and can therefore be treated separately as a perturbation one of the other. Observations indicate that after transcription only a sub-population of RNA molecules are in the active conformation and that inactive and active populations are separated by energy barriers sufficiently high so that interconversion between them does not occur under normal reaction conditions [14]. Among the molecules that are able to fold, it is possible to make another distinction between the molecules that reach the folded state directly, taking a very short time, and the molecules that reach the folded state much slower. In particular, small RNA molecules reach their native state without being trapped in misfolded structures, while long molecules are trapped more easily with increasing chain length [17]. Mutation studies on the tetrahymena group I ribozyme [18] reveal how the wild type RNA has a native-like kinetic trap and an additional slow step that also appears to be a trap. High activation enthalpy and low activation entropy were used as indications of the presence of a kinetic trap in the folding path. The high activation enthalpy indicates that bonds must be broken in order to continue folding. This shows that the view of RNA folding as a sequential process holds only as a first approximation, at least for some large molecules that still need rearrangements at the level of the secondary structure. At different temperatures the folding path seems to change with the molecules proceeding on an alternative slower path at low T.

Formation of tertiary interactions is thought to be rate determining for the folding of large RNAs. The fraction of RNA molecules that fold correctly during transcription is sensitive to changes in sequence so that even single point mutations can significantly increase or decrease the probability of folding. Mutations that accelerate the folding of the RNA molecule were found to be clustered in the region of the magnesium ion

binding site, suggesting that this structure has an role in nucleating folding [18].

6 Metal Ions and Water

In the absence of metal ions all known complex RNA folds form most of their secondary structure, but little, if any, of their tertiary structure [12]. Both metal ions and water can be considered as intrinsic parts of RNA 3D architecture.

While the majority of cations, especially monovalent ions like Na^+ , are delocalized, contributing to non-specific counter ion condensation, some ions occupy specific binding sites precisely defined by the 3D folding of the molecule. These ion binding sites are located at local minima in the electrostatic field created by the charges on the RNA atoms. Some divalent ion binding sites are pre-formed sites, i.e. the site exists in the absence of the metal ion and the structure of the site doesn't change upon binding to it. Some other metal ion binding sites are formed only after or during the formation of a tertiary structure, like, for example, during the formation of a pseudoknot.

Specific pockets for the binding of divalent ions are formed in loops and bulges, where the RNA backbone folds back on itself, bringing phosphate groups in close proximity. Not only backbone atoms are responsible for ion binding sites, electronegative atoms of the bases also contribute to specific metal ion binding sites in RNA architectures. This manifests especially in the deep groove regions where the electrostatic field of regular helical RNA is perturbed by non-canonical base pairs, like in the presence of a G·U wobble pair followed by a Y·G pair. Shallow groove G·A mismatches are another example of non-canonical base pair associated with cation binding sites.

Even though the majority of metal ion binding sites is for divalent ions, there are also cases of monovalent ion binding pockets. AA platforms contain a specific binding site for monovalent metal ions as an integral part of their structure. Since adenosine platforms are key elements of tetraloop receptors, site-specific binding of monovalent ions is also essential for correct folding.

The stability of tertiary structures exceeds that of any of the constituent subdomains only above certain concentrations of magnesium ion, indicating that this metal ion is essential for stabilizing the 3D structure. The cooperativity of the two-state pro-

cess, with melting of all subdomains simultaneously, is pronounced at high Mg^{2+} concentrations, whereas at low concentrations the melting occurs sequentially and independently in the domains according to their respective stabilities [14]. In the case of P5abc (see Section 8), the amount of folding increases with Mg^{2+} concentration and saturates at about 80% for concentrations larger than millimolar. A small amount of unfolded species are always observed.

In general, divalent ions affect the tertiary structure much more than the secondary, nevertheless the secondary structure of 56-nt P5abc subdomain in RNA in the absence of magnesium ions is found to be significantly different from the X-ray secondary structure [19]. This suggests that the presence of Mg^{2+} causes some rearrangement in the least stable parts of the secondary structure. The tertiary interactions stabilized by the presence of the magnesium ion not only change the 3D arrangement, but also change some base pairing.

Stable hydration patterns in surface depressions pockets and in the grooves of double-stranded RNA also contributes to the overall stability of the architecture. In tRNA a regular hydration pattern has been observed around the backbone in double-stranded regions, where water molecules bridge successive phosphate groups of each strand [12, 20]. The preferred binding of water at phosphate groups is due to both hydrogen bonding and electronegative potential around these sites. Like metal ions water molecules occupy electronegative pockets, thereby stabilizing the folding of the chain. Single binding water molecules form hydrogen bonds between unoccupied polar groups of the bases in many mismatches.

7 Predicting Secondary Structure Formation

Two techniques commonly used in predicting RNA secondary structure are phylogenetic comparison and thermodynamic stability.

In phylogenetic comparison many homologous sequences, corresponding to evolutionary variation of a particular RNA molecule, are first aligned and then searched for regions capable of base pairing. Covariance of nucleotides establishes which regions are involved in base pairing and which are not. The analysis of the molecules from organisms whose primary sequence differs by 20-40% give the best results. This method

cannot provide information about regions of secondary structure that are conserved. Since it strongly depends on the experimental information contained in the data base, more than on physical considerations and on modelling schemes, this approach will be no longer considered in the following discussion.

The second technique consists in the somewhat more physical approach of energy functional minimization. In thermodynamic stability studies, computer algorithms predict structures by calculating the free energies from all possible base pairing schemes and find the secondary structure that corresponds to the energy minimum. Algorithms that find several configuration of minimal energy (or energies close to the minimum) are preferred for several reasons: because base pair energies have large uncertainties, because tertiary interactions may stabilize a secondary structure that is not calculated to have the lowest energy, and because RNA molecules may not form a single secondary structure, but may instead have several structures in equilibrium [10].

Free energies are calculated from experimentally determined parameters using nearest-neighbor models for the regions which are base paired. Free energies for loop regions are harder to quantify. In the early models loop free energy was assumed to depend only on the number of nucleotides in the loop, using therefore only the entropic contribution to the free energy of formation. This approach can only be considered as a crude approximation, since we are now aware of examples of loops, like the tetraloops, whose energetic strongly depends on the sequence, due to the formation of non-canonical pairing. Regarding junctions, typical algorithms assume that their free energy depends on the number of stems and on the number of unpaired nucleotides within the junction only.

Let's analyze in more details the energetic of the formation of secondary interactions. The formation of a double stranded region occurs in two step: the formation of the first base pair (initiation), and the formation of subsequent pairs (propagation). The initiation of a base paired region in a single stranded RNA molecule involves the formation of a loop, and therefore implies a great loss in entropy. On the other hand propagation mainly involves an enthalpy gain. The authors of [21] propose to introduce a free energy of initiation as

$$\Delta G = -2.3 RT \ln(\gamma_m) \tag{1}$$

where γ_m is the probability of formation of a loop of m bases and depends on the identity and number of bases in the loop. This is clearly an entropic term.

For the free energy of propagation they propose

$$\Delta G_\alpha = \Delta H \left(1 - \frac{T}{T_\alpha} \right) \quad (2)$$

where T_α is defined as the melting temperature of a polymer entirely composed by bases of kind α ($\alpha=A\cdot U$ or $C\cdot G$), and ΔH is an experimentally determined quantity. Estimating the various contributions of helical content, loops and bulges, the free energy needed to form a secondary structure relative to a single strand is

$$\begin{aligned} \Delta G = & + N_{AU} \Delta H \left(1 - \frac{T}{T_A} \right) + N_{GC} \Delta H \left(1 - \frac{T}{T_G} \right) + \\ & - \Delta H \left(1 - \frac{T}{T_{\infty,m}} \right) - 2.3RT[B - 1.5 \ln(m + 1)] \end{aligned} \quad (3)$$

where the enthalpy of formation of one base pair, ΔH , is taken to be -8 kcal/mol. The first two terms are the free energies for adding N_{AU} A·U base pairs and N_{GC} G·C base pairs. The third term takes into account the fact that if you consider stacking interactions, the free energy of a double stranded region depends on $N-1$ rather than N nucleotides. The average value of 1.8 kcal/mol is used for this term. The fourth term is the right hand side of equation 1, with the prescription that γ_m is independent of the sequence and that the end-to-end distance of a strand of m nucleotides follows a Gaussian distribution characterized by the parameter B to be estimated.

$$\gamma_m = (m + 1)^{1.5} e^{-B} \quad (4)$$

Using equation 3 a stability number is assigned to helices, loops, and bulges. The stability number for a given RNA secondary structure is the sum of the contributions of all loops, bulges and helices. Stable structures have positive numbers measured in units of the free energy of formation for an A·U base pair. The structure with the highest number is the most stable.

More recent models for evaluating free energies of secondary structures explicitly take into account both hydrogen bonding and staking interactions when considering base

pairing. Loop energies comprise an entropic term for loss in conformational freedom, like the model by Tinoco, and other terms that account for mismatched pair stacking, coaxial helix stacking, single base stacking [9, 22]. The most recent and promising methods for predicting RNA folding tend to combine all possible information coming from both energy minimization and from phylogenetic analysis through covariation. Having seen how it is possible to assign energies to different configurations of the molecule, we can now turn to discuss different algorithms to implement the search for the configuration that minimizes this energy.

The approach now widely used to determine secondary structures in RNA molecules was introduced in 1980 by Zuker [23, 11]. It is called dynamic programming approach, and it is based on the assumption that the optimal secondary structure for a sequence can be found by first determining the optimal structure for each part of the sequence. He proposes to lay down very simple rules that using information available from different sources, from reactivity of certain nucleotides, to data on hydrolysis, and even phylogenetic data, assign an energy to each possible configuration. In the graphical representation of an RNA molecule, all nucleotides are drawn in a circle, or in closely related figure, and base pairing is represented by straight lines connecting two sites on the outer edge of the figure [refer to Figure 4]. An admissible structure is defined to be any planar region bounded on all sides by edges. Single strong constraints must be introduced to ensure planar unknotted appearance of the structure, i.e. no $i < k < j < h$ with i paired with j and h paired with k . This constraint is the key to most mathematical and computer work done on secondary structures since it ensures that all structures to admit a simple decomposition into sequentially analyzable substructures. The free energy of a structure is associated with the regions between bonds. A face with a single interior edge is a hairpin loop; faces with two interior edges separated by a single exterior edge on both sides are stacking regions; if they are separated by a single exterior edge on one side, but more on the other side they are bulges, otherwise they are internal loops; a face with three or more interior edges is a bifurcation loop or junction. The energy of a structure is the sum of the energies of all its faces.

The mathematical technique consists in computing two possibly different energies for each subsequence from monomer i to monomer j , S_{ij} , for a given RNA sequence.

For all pairs (i, j) where $i < j$, $W(i, j)$ is the minimum free energy of all possible admissible structures formed from the subsequence S_{ij} . $V(i, j)$ is the minimum free energy of all possible admissible structures formed from S_{ij} under the constraint that i and j are base paired with each other. $V(i, j)$ and $W(i, j)$ are computed recursively, first for all the pentanucleotide subsequences (smaller loops would violate $j - i < 3$), and then for all successively larger and larger subsequences. The recursive algorithm works by adding one nucleotide at the time to a sequence and by observing what is the best structure at each step. The last number to be computed, $W(1, N)$ is the desired answer, but the work done to compute it has also produced the minimum energy of an admissible structure for any subsequence of S .

The energy function plays a wider role than simply defining energies from thermodynamical studies, it is also used to enforce certain topological and folding rules. Base pairing can be forced by assigning very large negative energies to adjacent faces. The energy function can be used to incorporate all the extra information available on that sequence such as information on chemical modification, enzyme accessibility and so on. To exclude some configurations known to be impossible from chemical and stereochemical considerations, which are typically many, it is sufficient to assign them infinite energy, instead of formulating more complex rules that prevent them from forming from the beginning. In general, most of these constraints can be formulated in terms of thermodynamic instability of the resulting structure. The structure determined with this method is not necessarily unique and still needs to be tested to see how meaningful it is. One important criterion to see if a proposed base pairing region is valid is to check if the secondary structure of the region is preserved in other RNA molecules of related organisms.

The algorithm just presented is explained in more rigorous mathematical terms in [11] introducing the concept of k -cycles. The $k - 1$ pairs and u unpaired terms accessible from the pair (i, j) constitute the k -cycle closed by (i, j) . It is possible to show that no term belongs to more than one k -cycle simultaneously, so that every term is exactly external or it belongs to a stacked pair, a hairpin, a bulge, an interior loop or a multiple loop. The underlying hypothesis is to be able to decompose the sequence S into disjoint substructures with k -cycles S_1, S_2, \dots, S_t and that the energy is given by $E(S) = e(S_1) + e(S_2) + \dots + e(S_t)$ where $e(S_i)$ is the energetic contribution of cycle

S_i . The empirical knowledge required is the free energy contribution of each type of k -cycle. Only stacked pairs contribute negative energies and provide stability to the structure, external bases do not contribute. Non W-C base pairs can be avoided by making them prohibitively expensive in terms of free energies.

An approach alternative to the one introduced by Zuker, that allows to identify pseudoknots and triples, consists in constructing a graph in which each vertex corresponds to a base in an RNA sequence and potential base pairing interactions are represented by edges that connect the vertices, like in the graph used by Zuker, but to consider as an allowed structure each structure in which each vertex is visited at most once, without imposing constraints of planarity [24]. To each edge is assigned a weight which quantifies the strength of the evidence for that base pair's existence in the folded molecule. Solving the problem of finding the best matching, i.e. a subgraph in which no vertex is connected with more than one other vertex, is known as the MWM problem in graph theory [25]. Since it poses no restriction on planarity the algorithm can be used to predict pseudoknots and other tertiary interactions. MWM is constructed iteratively by first finding maximum weight matching consisting of one edge, than finding the maximum weight matching of two edges and so on, and by stopping the expansion in number of edges when the total weight cannot be further increased. An RNA structure that contains base triples may be represented by a 2-matching, a graph in which no vertex is connected with more than two other vertices. MWM is constructed in $O(N^3)$ time. Its success depends on how potential base pairs are scored. The principles on which to assign the scoring of each pair can be the same as the one used by Zuker, including both thermodynamical and phylogenetic information. A base known to be in a single stranded region can be enforced in MWM folding by assigning zero weight to every edge incident on a vertex that represents an unpaired base. A base known to be paired with a particular other base can be enforced by modifying the folding graph so that the edge representing a verified pair receives a positive score while all other edges incident on those bases receive weights of zero. As for the preceding approach, some kind of output filtration must be applied. It has been observed that when true base pairs are added to a graph they tend to remain stable in the graph, while spurious pairs tend to arise as the result of one or more rematching events. So, one possible way to filter the outcome is to monitor

the intermediate matchings and disregard unstable pairings.

MWM seems to be best suited to fold sequences for which a previous multiple alignment exists, so that scores may be assigned to possible base pairs by comparative analysis [24, 26]. So far the best working algorithms are energy minimization algorithms, but they have the limitation of the nesting condition, planarity, which doesn't allow to detect tertiary interactions. A recent reformulation of the original algorithm by Zuker (MFOLD) shows how this can be overcome at least for pseudoknots [26]. Let's restate the nested algorithm by Zuker under a new formalism that will allow for a generalization which would hold also for pseudoknots.

$vx(i, j)$ is the score of the best folding between position i and j , provided that i and j are base paired with each other. $wx(i, j)$ is the score of the best folding between position i and j regardless of whether i and j are paired or not. The recursion for vx includes contributions due to hairpins, bulges, internal loops and multiloops. Define an irreducible surface as a surface such that if a hydrogen bond is broken, there is no other surface contained inside it. The order of an irreducible surface (IS) is given by the number of secondary interactions, which is equal to the number of wavy lines in this graphical representation shown in Figure 13. A hairpin is a $O(1)$ IS, bulges and internal loops are $O(2)$ ISs and multiloops are $O(3)$ or more. For nested configurations an IS is equivalent to a k-cycle defined before, but the ISs are more general and include also non-nested structures. Recursion for vx is an expansion in ISs of successively higher order [Figure 14].

To make this approach a computationally practical algorithm, the expansion has to be truncated at some point. The simplest truncation is $O(0)$ in which none of the ISs are given any specific score and only base pairs count. In this case

$$vx(i, j) = B + wx_I(i + 1, j - 1) \quad (5)$$

where wx_I is similar to wx with the specification that it occurs inside a base pair. wx_I is used to truncate the recursion in vx , while wx is used only when there are no external bases. The next order of complexity is a truncation of order $O(2)$. Hairpin loops, bulges, internal loops are treated with precision by some scoring function, while multiloops are treated in an approximated form. This is the original nested algorithm previously described in [11].

Now we'll see how this formalism can be easily generalized to include pseudoknots.



Figure 13: Graphical representation of different kinds of irreducible surfaces. In blue a regular double stranded region; in yellow a bulge loop; in red a multiloop; in green an internal loop. On the right hand side of the picture is the representation of a simple pseudoknot.

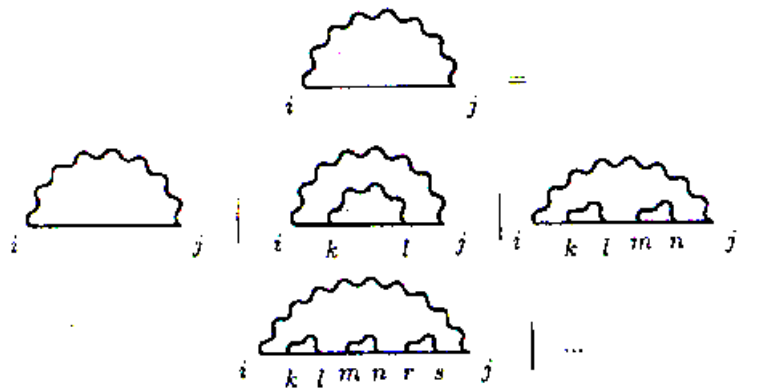


Figure 14: Expansion of $vx(i, j)$ in terms of irreducible surfaces of progressively higher order.

Pseudoknots are non-nested configurations and cannot be described by wx and vx alone. It is therefore necessary to introduce gap matrices, $whx(i, j; k, l)$, or one-hole matrices, as a generalization of vx and wx . Graphically it can be seen that a pseudoknot can be described by putting together two gap matrices, represented by half donuts, with complementary holes. $whx(i, j; k, l)$ is the graph that describes the best folding that connects segment (i, k) with (l, j) where $i < k < l < j$ such that the relation between i and j and k and l is undetermined. There are four such matrices depending on the relation between i and j and k and l . When there is no hole $whx(i, j; k, l) = wx(i, j)$.

A non gap matrix can be obtained by combining two gap matrices together, therefore one more diagram with two gap matrices can be added to the expansion for vx and wx . The recursion becomes an expansion in the number of gap matrices needed to represent the configuration. To the second order in the expansion, a non-solvable configuration is one that requires diagrammatic topologies that involve 3 or more gap matrices. A solvable configuration can be decomposed into the sum of gap matrices according to the rules provided for the recursion.

The additional parameters needed in order to include pseudoknots, are the score for a pair in a non nested multiloop, a generic score for generating a non-nested multiloop and a score for generating an internal pseudoknot.

8 Stretching Molecules by Mechanical Force

A series of interesting experiments carried on by the group led by C. Bustamante explored the behavior of long linear molecules under the influence of a stretching force [27, 28, 29, 30]. The authors have been studying the behavior of different kinds of molecules, and recently they analyzed also RNA, studying the response to stress of molecules of different tertiary structure complexity [30]. Their results are therefore very useful in trying to better understand the dynamic of folding. The technique they use is applicable to any long linear molecule, indeed the first studies involved DNA and Titin, which is a muscle protein responsible for contraction. In order to understand the kind of analysis and information derivable from these experiment, the discussion will include a brief presentation of the previous studies on these two

molecules [27, 28, 29].

Mechanical measurements could reveal the molecular mechanics responsible for the elastic response of the molecule over a full range of forces and extensions. After attaching one end of the molecule to a substrate and attaching a magnetic bead to the free end of the molecule, a magnetic field is turned on [27]. A combination of magnetic and hydrodynamic force displace the bead and extend the molecule along an angle θ relative to the direction of the magnetic field. To determine the tension in the molecule for each bead position it is necessary to know the maximum magnetic force acting on the bead. This is determined experimentally using Stokes' law $F = 6\pi\eta v$. The force stretches the molecule as each "segment" of the polymer tends to align with that force. On the other hand, the polymer residues oppose to alignment due to their thermal fluctuation. To an extended degree the molecule opposes to the stretch because of the loss in entropy.

The deformability of the molecule under stress is what gives rise to an enthalpic component of elasticity. It is not just a mere rearrangement of one segment with respect to another, but the segment itself can change shape. The enthalpic contribution is therefore associated with permanent small bends or local curvature of the molecule axis and it involves much larger deviations from the equilibrium shape than those caused by thermal fluctuations. These deformations become evident when the normal contour length of the molecule is approached or exceeded. Smaller overstretching forces may be required at low ionic strengths because the electrostatic repulsion between the phosphates favors the longer extended state.

Using this approach the authors identified and measured a dynamic persistence length of a single DNA molecule [27], and compared it with the values determined by bulk measures. They analyze it at different ionic concentrations, when DNA should be more stiff or more flexible. They find that the dynamic persistence length is more sensitive to ionic strength than the apparent value measured in bulk experiments.

In a different experiment they analyze how single and double stranded DNAs respond to overstretching, i.e. stretching over the normal contour length, allowing for strong enthalpic effects [28]. For double stranded DNA extensions below the contour length display an entropy driven behavior with the force rising rapidly as the contour length is approached. Then, suddenly, the molecule overstretches generating a transition

over a very narrow force range. This transition is narrower than thermal denaturation of double stranded DNA. Overstretching appears to be a highly cooperative reversible transition. The model proposed in order to explain this transition involves the unwinding of the two strands to form an unstacked parallel ladder. However, given that stacking interactions in single stranded DNA are known to be non-cooperative, the authors suggest that the cooperativity might arise by the propagation of changes in the state of hydration or in the ionic atmosphere, or both. Often, during relaxation, the force vs. extension curve displays hysteresis, and certain molecules are permanently altered after a few cycles. The single stranded DNA behaves differently, especially at low extensions. However the two curves are asymptotic to the same length at high forces.

In the experiment with the Titin molecule [29], the authors are interested in testing the validity of the WormLike Chain (WLC) for this muscle protein. The WLC describes the chain as a deformable continuum rod of persistence length A . The end-to-end distance z is related to the external force F and to the contour length L by

$$\frac{FA}{kT} = \frac{z}{L} + \frac{1}{4}\left(1 - \frac{z}{L}\right)^2 - \frac{1}{4} \quad (6)$$

Plots of $f^{-1/2}$ vs. z revealed that Titin does not behave as a WLC throughout the entire stretch-release cycle, but its behavior deviates from that of a WLC at high force during stretch, and at low force during release, indicating the onset of a structural transition. They propose this transition involves force-induced unfolding and refolding of the molecule. Again, the system displays hysteresis that could be accounted for by considering that if the rate at which the molecule is stretched and released exceeds the rate of unfolding and refolding of the molecule at equilibrium at that extension, then, at the end of the cycle, there will be some molecules which have not refolded. Stopping short of the transition in either directions abolishes the hysteresis. In this case also, successive cycles led to progressive deterioration of the molecule causing permanent denaturation.

Recently the same group followed the folding and refolding trajectories of individual RNA molecules [30]. One end of the molecule is held in a force-measuring optical trap while the other is linked to a piezo-electric actuator through a micropipette. They performed the experiments on the RNA molecules P5ab, P5abc Δ a, P5abc [Figure

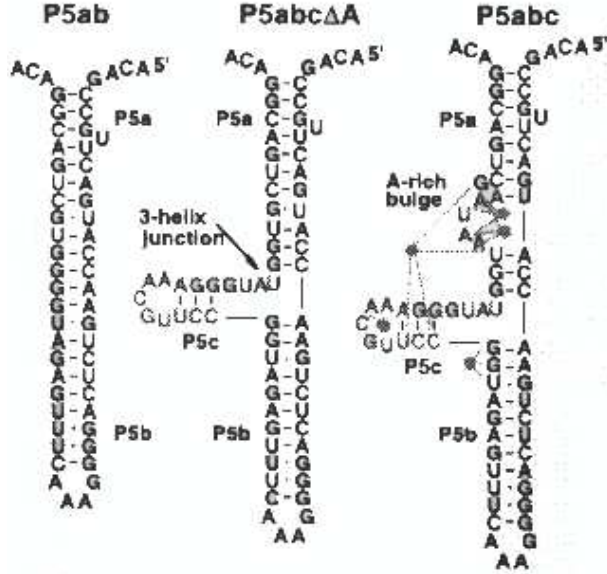


Figure 15: The three RNA molecules P5ab, P5abc Δ a, P5abc. Notice the absence of tertiary long range interactions in P5ab and in P5abc Δ a, while P5abc exhibits the interaction of the A-rich bulge and the hairpin mediated by the metal ion.

15].

P5ab is a small planar molecule that doesn't have any tertiary contact. This molecule is switched to the folded state, and viceversa, in less than 10 ms and doesn't show any intermediate states along the process. Forward and reverse process nearly coincide, indicating a condition of thermal equilibrium. A plot of the fraction of unfolded molecules vs. force is fit well by the statistic of a two state system in an external field at finite temperature. A ratio of the average lifetimes of the molecule in the two states yields the equilibrium constant $K(F)$ for that force. The sensitivity of RNA hopping between the folded and unfolded forms is determined by the force-dependent length difference between the two configurations $\Delta x(F)$, where $\Delta x(F)$ satisfies

$$\frac{d}{dF} \ln K(F) = \frac{\Delta x}{kT} \quad (7)$$

The logarithm of the mechanical folded/unfolded rate, $K_{f \rightarrow u}$, appears to be a linear function in the external force

$$K_{f \rightarrow u}(F) = C e^{\frac{F \Delta x_{f \rightarrow u}}{kT}} \quad (8)$$

where C is a proportionality constant. The position of P5ab transition state on the reaction coordinate, determined from the slope of the $\ln(K)$ vs. F , is equidistant from the unfolded and folded states.

P5abcΔa has a 3-helix junction structure. A force hysteresis appears indicating a loading rate which is faster than the slowest relaxation process of the molecule. The overall activation barrier is larger than that of P5ab, resulting in a slower kinetics.

P5abc has the most complex structure among the three. Its tertiary structure is stabilized by a magnesium ion that forms a metal-ion core between an helix and an A rich bulge. The tertiary interactions formed around Mg^{2+} lead to substantial curve hysteresis. Most of the times the molecule unfolds suddenly at high force. Only for a small percentage unfolding occurs in three steps revealing 2 kinetics barriers. The sharp transition, which is peculiar to this molecule but not to the other two, must therefore involve the interaction between the metal-ion and the A-rich bulge. Removal of Mg^{2+} removes the kinetic barriers and folding/unfolding becomes reversible. In contrast to the all-or-none behavior of P5ab, refolding of P5abc, both with and without magnesium ion, has intermediate states. The unfolding rate and position of the transition state of the first barrier are obtained using

$$N(F, r) = e^{(C \frac{kT}{\Delta x} e^{(bF-1)})} \quad (9)$$

where N is the fraction of folded molecules and r is the loading rate. Apparently the non-local contacts in the electrostatic core of RNA are responsible for the cooperative unfolding behavior under locally applied mechanical forces.

References

- [1] E.Weshof, P.Aufinger, *Encyclopedia of Anal.Chem.*, R.A.Meyers (Ed.), John Wiley and Sons Ltd, Chichester, p.5222 (2000)
- [2] J.Watson, N.Hopkins, J.Roberts, J.Argetsinger Steiz, A.Weiner, *Molecular Biology of the Gene*, The Benjamin/Cummings Company, Menlo Park, California, 1987 fourth edition
- [3] A.Bloomfield, M.Crothers, I.Tinoco, *Nucleic Acids. Structures, Properties, and Functions*, University Science Books, Sausaloto, Calofornia 2000
- [4] R.Batey, R.Rambo, J.Doudna, *Angew.Chem.Int.Ed.* **38**, p.2326 (1999)
- [5] E.Westhof, V.Frithch, *Structure* **8**, p.R55 (2000)
- [6] B.Masqyuda, E.Westhof, *RNA* **6**, p.9 (2000)
- [7] N.Leontis, E.Westhof, *Qart.Rev.Bioph.* **31** p.399 (1998)
- [8] E.Tosten ???? , Ph.D. thesis at DTU, 1999
- [9] M.Zuker, *Curr.Op.Struct.Biol.* **10**, p.303 (2000)
- [10] I.Tinoco, *Prog.Nucl.A.Res and Mol.Biol.* **41**, p.131 (1991)
- [11] M.Zuker, D.Sankoff, *Bull.Math.Biol.* **4**, p.591 (1984)
- [12] T.Hermann, D.Patel *J.Mol.Biol.* **294**, p.829 (1999)
- [13] M.Zuker, *Science* **244**, p.48 (1989)
- [14] P.Brion, E.Westhof, *Annu.Rev.Biomol.Struct.* **26**, p.113 (1997)
- [15] I.Tinoco, C.Bustamante, *J.Mol.Biol.* **293**, p.271 (1999)
- [16] T.Gluick, D.Drappers *J.Mol.Biol.* **241** p.246 (1994)
- [17] D.Thirumalai, S.Woodson, *Acc.Chem.Res.* **29**, p.433 (1996)

- [18] M.Rook, D.Treiber, J.Williamson, *J.Mol.Biol.* **281**, p.609 (1998)
- [19] M.Wu, I.Tinoco, *Proc.Natl.Acad.Sci. USA* **95**, p.11555 (1998)
- [20] E.Westhof, P.Dumas, D.Moras, *Biochimie* **70** p.145 (1988)
- [21] I.Tinoco, O.Uhlenbeck, M. Levine, *Nature* **230** p.362 (1971)
- [22] J.SantaLucia, *Proc.Natl.Acad.Sci. USA* **95** p.1460 (1998)
- [23] M.Zuker, P.Stiegler, *Nucleic Acids Res.* **9**, p.133 (1981)
- [24] J.Tabaska, R.Cary, H.Gabow, G.Stormo, *Bioinformatics* **14**, p.691 (1998)
- [25] R.Cary, G.Stormo, *Proceedings of the third International Conference of Intelligent Systems for Molecular Biology*, AAAI Press, Menlo Park, California, p.75 (1995)
- [26] E.Rivas, S.Eddy, *J.Mol.Biol.* **285**, pp.2053 (1999)
- [27] S.Smith, L.Finzi, C.Bustamante, *Science* **258**, p.1122 (1992)
- [28] S.Smith, Y.Cui, C.Bustamante, *Science* **271**, p.795 (1996)
- [29] M.Kellermayer, S.Smith, L.Granzier, C.Bustamante, *Science* **276**, p.1112 (1997)
- [30] J.Liphardt, B.Onoa, S.Smith, I.Tinoco, C.Bustamante, *Science* **292**, p.733 (2001)